HHS Public Access

Author manuscript

Mol Neurobiol. Author manuscript; available in PMC 2020 October 01.

Published in final edited form as:

Mol Neurobiol. 2019 October ; 56(10): 7159–7172. doi:10.1007/s12035-019-1589-z.

Chemotherapy induced cognitive impairment is associated with increased inflammation and oxidative damage in the hippocampus

Ciara Bagnall-Moreau[1,2], **Sovira Chaudhry**[1], **Kaliris Salas-Ramirez**[3], **Tim Ahles**[4], **Karen Hubbard**[1,2]

[1]Biology Department, The City College of New York, New York, NY 10031;

[2]The Graduate Center of City University of New York, New York, NY 10016;

[3]Department of Molecular, Cellular and Biomedical Sciences, CUNY School of Medicine, New York, NY 10031;

[4]Department of Psychiatry and Behavioral Sciences, Memorial Sloan Kettering Cancer Center, New York, NY, 10022.

Abstract

Increasing evidence indicates that chemotherapy results in long-term effects on cognitive dysfunction in some cancer survivors. While many studies have established the domains of cognition and corresponding regions in the brain most affected, little is revealed about the potential molecular mechanisms that mediate these adverse changes after treatment. The effects of chemotherapy on the brain is likely attributed to various mechanisms including oxidative stress and immune dysregulation, features that are also reminiscent of cognitive aging. We have investigated the effects of the cocktail doxorubicin and cyclophosphamide (AC-chemo) in a surgical ovariectomized, rodent model of the cognitive effects of chemotherapy. In this study, we address whether the levels of pro-inflammatory cytokines and oxidative stress- responsive gene markers are altered in the CNS of rats treated with systemic AC-chemo. We further evaluated the levels of nucleic acids modified by oxidative stress in the hippocampus using both immunohistochemical and northern blotting techniques with a monoclonal antibody against 8-hydroxyguanosine (8OHG) and 8-OHdG base lesions. We demonstrate that ERK 1/2 and JNK/SAPK signaling activities are elevated in the hippocampus of AC-chemo rats. The levels of pro-inflammatory, oxidative stress-responsive and RNA/DNA damage markers were also higher in drug-injected animals relative to saline controls. The results indicate that the effects of AC chemotherapy are associated with oxidative damage and a global stress response in the

Corresponding Author: Dr. Karen Hubbard, Department of Biology, The City College of New York, New York, NY 10031, Tele: 212 650-8566, Fax: 212 650-8585, khubbard@ccny.cuny.edu.

Conflict of Interest

The authors declare that they have no conflict of interest.

hippocampus. These alterations in the molecular signature of the brain may underlie the processes that contribute to cognitive impairment after treatment.

Keywords

brain aging; chemotherapy; cognitive impairment; oxidative damage; MAPK signaling; neuro-inflammation

Introduction

Chemotherapy remains as an effective approach for the treatment of various cancers. Despite the efficacy of treatment on improving survival in patients, these methods often lead to long term complications that impact the quality of life. Systemic delivery of chemotherapeutics is associated with adverse effects in some non-central nervous system malignancies. There is a growing concern that cancer and cancer therapies elevate the risk of frailty and chronic comorbidities in survivors and is linked to an accelerated molecular ageing phenotype in some patients [1, 2]. The prevalence of this chemotherapy-related cognitive impairment (CRCI) is reported to range from 17%– 75% of patients during and for 1–2 years following treatment, although a subset of individuals (35%, [3]) experience deficits that persist for decades following treatment [4]. In the United States alone there are 15.5 million cancer survivors, which suggest that millions will likely face long- term cognitive difficulties stemming from cancer and the related treatments.

Several candidate mechanisms have been hypothesized to contribute to CRCI, which indicates a need for more studies to characterize the role of these various factors [5, 6]. The evidence from the literature supports a neurobiological basis for cognitive changes after treatment although the specific pathways involved are not very well defined and are often challenging to assess [7, 8]. It is important to note that chemotherapy is considered a risk factor for cognitive impairment and the extent of dysfunction may be influenced by treatment regimen and the biological mode of action by these cytotoxic compounds [9]. In particular, the inclusion of anthracyclines such as doxorubicin and/or in combination with other drugs have been proven to reduce disease progression and improve patient outcome [10]. The precise mode of action varies depending on the type of anthracycline, but generally drugs among this class can interact with topoisomerase and intercalates between DNA base pairs leading to double strand breaks [11]. Furthermore, anthracyclines exhibit a redox cycling profile that generates robust levels of free radicals and reactive oxygen species, a mechanism associated with cardiomyopathy and other cardiac complications [12]. Several clinical studies have demonstrated alterations in brain functionality (e.g. fMRI) and cognitive impairment (e.g. neuropsychological testing) in breast cancer patients that were treated singularly with anthracyclines or in combination with other drugs [13–15]. A recent study found that patients receiving anthracycline- based treatment exhibited lower verbal memory and significantly lower default mode brain network connectivity when compared to healthy controls and patients who received non-anthracycline regimens [16]. Therefore, anthracyclines such as doxorubicin may carry an increased risk for cognitive dysfunction and neurotoxicity.

Human clinical studies have offered invaluable insight into the complexity of CRCI although the interpretation of many of these findings are often complicated by the presence of comorbid conditions in cancer survivors, independent of treatment status. Animals studies have greatly expanded the biological knowledge of CRCI and have facilitated the design of controlled experiments to address various candidate mechanisms [7]. Clinical and animal studies indicate that various treatments cause alterations to brain morphology and /or brain activation [8]. These changes are proposed to be mediated by direct effects on specific CNS cell populations (i.e., neuronal and glial progenitors) or indirectly through neuroinflammation and damage to the brain vasculature [17]. A number of translational studies conducted with rodents have also established the cognitive domains that are affected by various chemotherapy treatments and have identified promising behavioral and pharmacological interventions for reducing the adverse effects of treatment [7][18].

Due to the limited transport of many agents across the blood brain barrier, the effects of chemotherapy in the brain could be mediated in part through neuroinflammatory mechanisms. Several animal models have corroborated the human clinical studies showing an increase in the levels of cytokines or inflammatory brain macrophages following various treatments [19–21]. For example, the elevation of circulating tumor necrosis factor alpha (TNFα) in rats after treatment with doxorubicin is a common pathway demonstrated to induce oxidative damage in the CNS and adverse effects on cognitive behaviors [22]. Alternatively, several agents directly induce oxidative stress as a mechanism of toxicity that can also cause damage to the components of normal cells and tissues [23]. Chronic inflammation and oxidative stress are key role players in the development of chronic disease conditions that are associated with advanced age. It is therefore plausible that adjuvant chemotherapy may further promote gerontogenic effects on several organ systems through these physiological mechanisms and lead to cognitive dysfunction in cancer survivors.

Previously we evaluated the effects of doxorubicin/ cyclophosphamide (AC) drug combination on cognitive behaviors in tumor-free female Sprague Dawley rats [24]. Ovary-intact and ovariectomized (OVX) animals were included as an experimental model for adjuvant ovarian suppression in breast cancer survivors [25]. The results of the behavioral testing demonstrated that AC chemotherapy impairs hippocampal -mediated cognitive processes in rats. Furthermore, this effect was independent of hormonal status as drug treatment in both intact and OVX animals show similar deficits in hippocampus-mediated behaviors. In the present work, we examine the effect of chemotherapy on markers of inflammation, oxidative stress and the antioxidant defense in the hippocampus as a potential mechanism by which cancer and its treatment affect cognitive functioning. Overall, the results show that systemic AC chemotherapy increases ERK and JNK, MAPK signaling activities, upregulates inflammatory cytokine and chemokine levels, and increases the mRNA expression of several oxidative stress-responsive genes in the hippocampus. Finally, we demonstrate that increased levels of oxidative nucleic acid damage markers were evident after treatment.

Materials and Methods

All experiments were conducted according to protocols approved by the Institutional Animal Care and Use Committee at The City College of New York. Ovariectomized (OVX) female Sprague Dawley rats at the age of 8–10 weeks were obtained from Charles River Rats were divided into two groups, vehicle and chemotherapy for subsequent molecular (n=6–7) or immunohistochemical (n=5) studies. Drug treatments were carried out as described previously [44]. Briefly, rats in the chemotherapy groups were intravenously injected once a week for three weeks with the combination of cyclophosphamide (40mg/kg; LKT Laboratories) and doxorubicin (4 mg/kg; LKT laboratories) prepared in 0.9% saline solution. The vehicle control animals were administered an equal volume of saline. One week following the last injection, rats were euthanized by decapitation for the collection of tissue for the biochemical analyses. Whole brains were rapidly removed and the hippocampus was isolated on ice from each hemisphere, flash frozen in liquid nitrogen and stored at −80° C until further processing.

Protein Extraction and Western Blot Analysis:

For protein extraction, brain tissue from one hemisphere of each animal was homogenized as described previously [44]. Briefly, tissue was lysed in ice-cold NP40 buffer (40mM Tris–HCl pH 7.5, 274 mM NaCl, 2 mM EGTA, 20% v/v glycerol, 50 mM NaF, 1 mM Na3VO4, 1mM beta-glycerophosphate, 1 mM PMSF, 2.5 mM sodium pyrophosphate, 1% NP-40, and protease inhibitor cocktail (Thermo Scientific) using a BioMasher single use homogenizer and clarified by centrifugation at 14,000 x g for 15 min at 4° C. Protein concentrations were determined using the micro BCA protein assay (Pierce) using bovine serum albumin as a standard according to manufacturer's protocol. Thirty micrograms of protein from the hippocampal and PFC brain tissue were loaded in each lane and electrophoretically separated on either 10% or 12% SDS- PAGE gels and transferred onto a PVDF membrane. The membranes were blocked in 5% nonfat dry milk for one hour at room temperature and subsequently incubated with specific primary antibodies overnight at 4°C. Following several washes, membranes were incubated for one hour with the appropriate HRP-conjugated secondary antibodies. The immune complexes were detected by the enhanced chemilluminescence (ECL) detection system (GE) and signal intensities were quantified by Image J using β actin as a loading control. The following antibodies were used for the biochemical studies: Phospho c-Jun S63 (D47G9) and total c-Jun (60A8); phospho ERK T202/Y204 (D13.14.4E) and total ERK; phospho SAPK/JNK T183/Y185 (81E11) and total SAPK/ JNK; phospho p90 RSK S380 and RSK1/2/3 were obtained from Cell Signaling Technology. Mouse monoclonal antibody against β actin (BA3R) was purchased from Thermo Fisher Scientific.

Rat Cytokine Arrays and Image Analysis:

Rat cytokine profiling was performed using a membrane -base sandwich immunoassay Proteome Profiler Rat Cytokine Array Kit (Panel A, R&D Systems). Hippocampal tissue lysates (400 micrograms total protein) from either saline or AC chemotherapy injected rats were mixed with a cocktail of biotinylated detection antibodies and incubated at room temperature for one hour. The lysate/antibody mixture was then added to membranes spotted

with capture antibodies and incubated overnight at 4° C. Membrane arrays were extensively washed to remove unbound antibodies and Streptavidin-HRP followed by addition of a chemiluminescent reagent mix. The membrane arrays were exposed to autoradiography film at several time points. Pixel densities from each membrane (n=6) were analyzed using the semi-automated Quick Spots image analysis software from Western Vision Software.

RNA Isolation and Quantitative Reverse Transcription Polymerase Chain Reaction (qRT-PCR):

Total RNA was extracted from the hippocampus of the remaining hemisphere from each animal in TRI Reagent (Invitrogen) according to the manufacturer's instructions and incubated with DNase I to remove contaminating genomic DNA. RNA quality was assessed by agarose gel electrophoresis and the concentration was quantified using the NanoDrop spectrophotometer. All RNA samples used in the study obtained A260/A280 ratios that ranged from 1.8 to 2.0. Total RNA samples (500ng) were heat denatured at 65° C for 5 minutes and immediately cooled on ice. Complementary DNA (cDNA) was synthesized using a random hexamer/ anchored oligo dT primer mix according to the Verso cDNA synthesis protocol (Thermo Fisher Scientific). PCR amplification of cDNA was carried out with Power Up SYBR Green Master Mix (Thermo Fisher) using gene specific primers (Table 1). PCR products were monitored using the Applied Biosystems 7500 Real-Time PCR System and amplicon specificity was confirmed by melt curve analysis. Fold changes in gene expression relative to saline controls was calculated using the comparative CT method, with reference to the housekeeping gene *GAPDH*. Statistical analysis for each target gene was performed on ΔCT values between saline and chemotherapy treated groups

Immuno-Northern Blot Analysis of RNA Oxidation 8-Hydroxyguanosine (8-OHG) adducts:

Three micrograms of total isolated RNA from the hippocampus were prepared in sample buffer (20 mM MOPS, 5 mM sodium acetate, 1 mM EDTA, 2.2M formaldehyde, 50%(v/v) formamide, and heat denatured at 65° C for 15 minutes. RNA samples were immediately placed on ice and mixed with tracking dye containing SYBR Safe (Thermo Fisher) before being loaded onto (.8%–1%) agarose gels prepared in 1X formaldehyde buffer (20mM MOPS, 5mM sodium acetate, 36 1mM EDTA, 2.2M formaldehyde) [45]. After electrophoresis, gels were visualized using a blue light illuminator to detect prominent ribosomal bands and to confirm equal loading. Capillary transfer of RNA onto positively charged nylon membranes (Biodyne B, Thermo Sci) were carried out in 20X SSC buffer overnight. Membranes were exposed to UV irradiation (Hoefer UVC500) in order to crosslink RNA to the filter. Transfer efficiency was confirmed by methylene blue (Alfa Aesar) staining. Transferred membranes were blocked for 1 hour in 5% bovine serum albumin in Tris buffered saline and 0.1% Tween 20 and then incubated in the primary monoclonal antibody 8-OHdG/ 8-OHG 15A3 (1:5000, Thermo Fisher) overnight at 4° C. After washing in Tris-buffered saline with Tween 20, membranes were incubated in horseradish peroxidase- conjugated mouse secondary antibody (1:3000) for 1h. Chemi-luminescent signals were detected using the SuperSignal West Pico Substrate (Thermo Scientific) and exposed to Clxsposure film (Thermo Scientific).

Dot Blot Analysis of 8-OHG adducts:

One microgram of unfractionated total RNA was heat denatured in a solution of 50% formamide/2.2 M formaldehyde according to the procedures of Brown, Mackey, and Du [46]. Denatured RNA samples were immobilized onto positively charged nylon membranes using the Bio -Rad microfiltration apparatus and crosslinked by UV irradiation. The membrane was blocked for one hour in 5% bovine serum albumin in Tris Buffered Saline and Tween 20 (TBS–T) and subsequently probed with the primary monoclonal antibody 8-OHdG/ 8-3;OHG overnight at 4° C. After washing in TBS-T, membranes were incubated with HRP–conjugated anti mouse secondary antibody and signals were detected by ECL as described above. Specificity of oxidized RNA was confirmed by preincubation of RNA with RNase prior to membrane blotting.

Immunohistochemical Analysis of OH(d)G adducts:

Brain tissue from a separate cohort of animals (n=5) were used to determine the levels of nucleic acid oxidation by semi-quantitative immunohistochemistry. The animals used in these studies were anesthetized with an overdose of pentobarbital and perfused transcardially with heparinized saline followed by 4% paraformaldehyde. Afterwards brains were post-fixed for 1 hour and placed in 20% sucrose/phosphate buffered saline solution. Brains were sectioned at 40 microns and were stored in a cryopreservative under −20° C until use.

Immunohistochemical procedures were conducted on paired free-floating coronal sections from the brains of saline and AC chemotherapy- injected rats. Heat-induced antigen retrieval was performed on slices using an antigen unmasking solution (Vector) and subsequently placed in 0.3% hydrogen peroxide solution to quench endogenous peroxidase activity. Sections were blocked with 3% goat serum with 0.4% Triton X-100 for 1 hour and then incubated with a mouse monoclonal anti 8–OHdG antibody (Thermo Fisher) overnight at 4° C. The omission of primary antibodies from the blocking solution served as a negative control. Biotinylated mouse secondary antibodies were added to sections for 1 hour and detection of antigen was carried out using a Vectastain ABC kit (Vector Laboratories) using 0.03% hydrogen peroxide and DAB substrate as a chromogen. Sections were mounted onto Superfrost coated slides, air dried overnight and dehydrated in increasing alcohol concentrations before being defatted in xylene and cover slipped in Permount mounting medium.

Photomicrographs were acquired from the regions of interest using a Zeiss Axioplan 2 microscope with Nikon NIS-Elements under standardized conditions including white balance. Images were exported as TIFF files and semi-quantitative analysis on the converted 8-bit images was carried out with the ImageJ software (NIH). A threshold level was set and applied to all images for comparison. The percent area occupied by signal in 5 fields of each region of interest was measured and the averages were compared between chemotherapy and saline-control groups.

To exclude the possibility that peroxidase quenching induced 8-OHdG adducts, the incubation of hydrogen peroxide was omitted prior to immunofluorescence procedures

conducted in parallel tissue slices. Sections were similarly blocked in 3% goat serum with 0.4% Triton X-100 for 1 hour and subsequently double-labelled with the anti 8–OHdG antibody and the neuronal marker anti-NeuN (Novus Biologicals) at 4° C overnight. After extensive washing in TBS, sections were incubated in Alexa-647 conjugated anti-mouse and Alexa-488 conjugated anti- rabbit secondary antibodies for 2 hours in the dark at room temperature. The sections were washed and cover slipped in fluorescence mounting medium (Dako) containing the nuclear marker 4', 6-diamidino-2- phenylindole (DAPI). Immunofluoresence images were obtained using a Zeiss LSM710 laser scanning confocal microscope.

Primary Culture of Rat Hippocampal Neurons:

Dissociated hippocampal neurons were prepared from 1 day-old postnatal Sprague Dawley rat pups (Charles River Laboratories) for *in vitro* neurotoxicity studies as described previously with modifications [47]. Isolated cells were initially seeded onto poly -D-lysine (100 μg/ml) coated 8-well chamber slides at a density of 1× 105 cells/well in a plating medium consisting of DMEM with 10% fetal bovine serum (FBS). After about 4 hours or when most cells attach, the plating medium was replaced with a Neurobasal medium supplemented with B27, Glutamax, and penicillin/ streptomycin (all Life Technologies). On day 3 post-plating, cytosine arabinoside (AraC, final concentration 1uM) was added to neuronal cultures to reduce glial cell proliferation. Cell cultures were maintained at 37°C in a humidified 5% CO_2 atmosphere chamber and half of the medium was exchanged every 3–4 days.

Evaluation of Oxidative Stress and DNA Damaging Effects of Doxorubicin in Hippocampal Neurons:

After 13 D.I.V. the culture media was switched to Neurobasal/ B27 supplement minus antioxidants (-AO). After a 1 h pretreatment with 100 μM acetyl L carnitine (ALCAR, Sigma), doxorubicin was added at a final concentration of 0.25 μM and cells were incubated in a humidified atmosphere of 95% air and 5% CO_2 at 37° C for 6 h. To evaluate the induction of reactive oxygen species (ROS) after drug treatment, CellROX Deep Red Reagent (5μM, Thermo Fisher) was added to wells for 30 min at 37° C. After washing with PBS, slides were fixed for 10 min in 3.7% paraformaldehyde and mounted onto coverslips using ProLong Gold Antifade Mountant with DAPI (Thermo Fisher). Fluorescent signals were detected using a confocal laser scanning microscope (LSM710; Zeiss). Images were subsequently analyzed with ImageJ software.

The expression of the DNA damage marker 8 OHdG was also examined in cells after doxorubicin exposure using immunofluorescence staining procedures. Neurons were cultured in chamber slides and treated as described above. Cells were then fixed in 3.7% paraformaldehyde for 15 min, permeabilized with 0.1% saponin for 15 min and blocked with 1% BSA in PBS with 0.25% Tween 20 for 30 min. Cells were incubated overnight in mouse anti- 8 OHdG (Thermo Fisher) and rabbit anti- Neun (Novus biological) primary antibodies in blocking buffer at 4° C. Antigen detection was performed using Alexa Fluor 488 and Alexa Fluor 633 conjugated secondary antibodies (Invitrogen). Slides were cover

slipped in ProLong Gold Antifade Mountant with DAPI (Thermo Fisher) and images were captured using the Zeiss 710 Laser Scanning Confocal Microscope.

Statistical Analysis:

All data was graphed using Microsoft Excel. Statistical analyses were performed with Graph Pad Prism 5.0 (GraphPad Software, Inc., San Diego, CA) by using a student's t test. Values were expressed as the mean ± SEM. Differences between groups were considered to be significant at a $P < 0.05$.

Results

Cytokine and chemokine levels are altered in the hippocampus of chemotherapy treated animals

Increases in oxidative stress as discussed previously may contribute to cognitive impairment through premature aging of the brain and is associated with an increase in inflammation. Clinical and experimental evidence indicate that pro-inflammatory cytokines may be mediators of chemotherapy-associated cognitive impairment, thus we sought to determine the levels of cytokines and chemokines following AC treatment. In the present study, the relative levels of various cytokines and chemokines were determined simultaneously using a membrane based antibody array (R&D, ARY008). The 29 cytokines included in the array is shown in Fig. 1b. Pixel density signals from duplicate spots were averaged and quantitative analysis of measurements indicate that the protein differences between saline and AC chemotherapy groups were not statistically significant (Fig. 1a,1c). However, increases of >1.5 fold was measured for IFN-gamma, IL-2, IL-3, IL-4, IL-6, IL-10, LIX, L-Selectin, MIG, MIP-1alpha, MIP-3alpha, VEGF, GM-CSF, ICAM-1, IL-1ra, IL-17, IP-10, and TNF-alpha in the hippocampal lysates of AC-chemotherapy treated animals (Fig. 1b). These observations indicate that AC treatment increases the level of several pro-inflammatory cytokines are consistent with reports from others [20].

Analysis of oxidative stress -responsive gene expression in the hippocampus

Since our studies showed an increased in inflammation, we then measured the expression levels of proteins known to have antioxidant activities. Using RT-qPCR analysis, the mRNA expression of antioxidant and oxidative-stress responsive genes were evaluated in the hippocampus. The relative levels of GPX1 (glutathione peroxidase 1), NFkB (nuclear factor kappa-light-chain-enhancer of activated B cells, p65 subunit), PRDX1(peroxiredoxin-1) and TNFα(Tumor necrosis factor alpha) were all significantly higher in AC chemotherapy groups relative to saline controls (Fig. 2). The levels of HO–1 (Heme oxygenase 1) were decreased in chemo- treated animals ($p < 0.05$, Fig. 2). While many of these proteins have altered levels of expression, we realize that further studies are needed to determine if enzymatic activities reflect the levels of expression observed.

ERK/MAPK and JNK/SAPK signaling is elevated in the brains of animals after AC chemotherapy treatment

In our earlier study, the phosphorylated levels of ERK/MAPK were found to be significantly higher in hippocampal lysates from OVX -AC chemotherapy treated groups relative to

OVX-saline control rats [24]. MAPK cascades are involved in a number of stress response signaling pathways in the CNS. To examine pathway specificity, the activation of the ERK/MAPK and the SAPK/JNK pathways and their (direct) substrates p90 RSK and c-Jun were measured. Significantly higher levels of activated (phosphorylated) SAPK/JNK (Thr183/Tyr185) were detected in the hippocampus of AC- treated rats relative to controls ($p<0.05$; Fig. 3b).

Furthermore, the phosphorylated levels of a downstream target of the JNK pathway, c-Jun were found to increase after treatment ($p<0.05$; Fig. 3c). The phosphorylation of ERK 1/2 was also increased in the hippocampus after chemotherapy ($p<0.05$; Fig. 3f). There were no changes in the relative activation of p90 RSK although overall RSK protein levels were significantly elevated in AC- chemotherapy groups ($p<0.005$; Fig. 3e). Thus, it appears that a global oxidative stress response is mounted on AC treatment and it is reflected in an upregulation of multiple MAPK pathways.

Oxidative damage in the hippocampus is associated with AC chemotherapy

DNA and/or RNA damage can be a direct consequence of oxidative stress. In the above studies, we observed an increase in the expression of inflammatory proteins and MAPK activation and suggest that oxidative damage may have occurred through AC administration. To address if systemic AC chemotherapy is associated with oxidative modifications to nucleic acids in the brain, the levels of the DNA/RNA oxidation marker 8–OH(d)G was evaluated in RNA isolated from the hippocampus of AC-chemotherapy treated rats. Immuno-dot blot analysis was performed on unfractionated total RNA (Fig. 4; See methods). Increased 8–OH(d)G immunoreactivity from AC chemo-treated groups was observed relative to the saline controls ($p<0.05$; Fig. 4a, 4b).

Immuno-northern blot (INB) analyses of 8–OH(d)G adducts were also performed on total RNA that was electrophoresed on a denaturing formaldehyde gel (Fig. 5a–c). The densitometric analysis of the oxidation marker indicates that AC chemotherapy treated animals exhibit significantly higher levels of oxidized 28S ribosomal RNA bands than saline- controls in the hippocampus ($p<0.05$; Fig. 5d).

The levels of 8–OH(d)G in the hippocampus were further validated using semi- quantitative immunohistochemical methods (Fig. 6a). Tissue section staining and image acquisition were performed in parallel for the entire set (n=5/group) using ImageJ software (NIH). Positive 8–OH(d)G staining was assessed initially setting a “threshold” through the thresholding tool and was applied to all images to be compared. Within each region of interest (ROI) in the hippocampus, the percent area occupied by 8–OH(d)G stain (brown) in 5 fields was measured. In AC chemotherapy- treated animals, increased neuronal staining for 8–OHdG was observed in various hippocampal brain regions (Fig. 6a). Semi-quantitative analysis of the staining patterns suggests a higher percentage of 8–OH(d)G area intensities in the CA1 and CA3 regions of the hippocampus relative to control animals ($p< 0.05$; Fig. 6b). Fluorescence microscopy further demonstrated that the cells immunolabelled with 8–OHdG also co-express neuronal specific marker NEUN (Fig. 6c). In Figure 6c, the CA1 pyramidal cell layer is depicted in the immunofluorescence images and demonstrate that 8–OH(d)G staining is primarily observed in neuronal cells types as noted by the colocalization with the

NEUN lineage marker. These modifications indicate that induction of oxidative stress by chemotherapy may be selective to specific cell populations, particularly neurons that exhibit a greater intrinsic vulnerability to stress [26].

ROS levels increase in hippocampal neurons treated with doxorubicin

The generation of free radicals and oxidative damage contributes to the toxicity of anticancer drugs in the brain and other noncancerous tissues [23]. In our previous paper, we demonstrated that chronic exposure to a common chemotherapy cocktail, cyclophosphamide and doxorubicin, impairs some forms of hippocampal dependent memories in rats [24]. Others have also observed that behavioral alterations in rodents administered doxorubicin alone are associated with enhanced proinflammatory cytokine production and oxidative damage in the plasma and brain [22, 27–29]. In this study, the levels of ROS were measured in an *in vitro* model of doxorubicin -induced neurotoxicity using a far-red photostable fluorogenic probe. As described previously, hippocampal neurons plated onto 8-well chamber slides were incubated in B27 -AO medium (antioxidant-free), exposed to 0.25 μM doxorubicin for 6 hours and subsequently labelled with 5 μM CellROX Deep Red Reagent. We did not find significant production of ROS in dissociated neurons exposed to low micromolar doses of cyclophosphamide in pilot studies (unpublished data), thus, we are presenting results studies in which neurons were exposed to solely to doxorubicin.

As shown in Fig. 7, a 0.25 μM exposure of doxorubicin led to a 3-fold increase in CellROX signal intensities (* $p<0.05$, compared to control). This significant increase in ROS levels by 0.25 μM Dox was mitigated by the pretreatment of neurons with 100 mM of acetyl-L-carnitine (# $p<0.05$, compared to Dox group). To address a consequence of elevated intracellular ROS in neurons, the expression of the DNA damage marker 8 OHdG was detected using immunofluorescence staining. Doxorubicin treated hippocampal neurons also exhibit strong nuclear staining by the 8OHdG antibody that is consistent with the increased ROS levels detected by the CellROX fluorogenic probe (Fig. 7c). The *in vitro* oxidative stress data presented here supports a potential mechanism of doxorubicin-induced cytotoxicity in neuronal cells.

Discussion

In the present study, we investigated the potential role of inflammation and the oxidative stress responses in AC (doxorubicin, cyclophosphamide) chemotherapy- induced cognitive impairment. The ovariectomized (OVX) rat is a model for surgically- induced ovarian loss and menopause. An overwhelming number of clinical studies on cognitive dysfunction in breast cancer patients address menopausal status and adjuvant endocrine therapy as contributory factors to CRCI, considering that hormone imbalance is documented to influence cognition [30]. We have previously assessed the behavioral and cognitive consequences of systemic AC chemotherapy in a rat model [24] as well as others using different rodent models [19, 31]. Overall, the present results indicate that an induction of inflammation and MAPK signaling is accompanied by oxidative damage to nucleic acids in the hippocampus of AC chemotherapy- treated rats.

The levels of various proinflammatory cytokines and chemokines are upregulated in hippocampal protein lysates of chemotherapy- treated animals (Fig. 1). Among these inflammatory regulators, IL-6 and TNFα are consistent with the peripheral cytokine biomarkers that have been observed in breast cancer patients during treatment and in both the plasma and CNS of doxorubicin injected rats [14, 21, 22, 32, 33]. Furthermore, the qRT-PCR data analysisin Fig. 2 showing an increase in the mRNA levels of TNFα and the transcription factor NFkB suggests that the activation of pathways leading to neuroinflammation are upregulated. The expression of several oxidative stress- responsive and antioxidant genes were also elevated in the hippocampus after treatment. Both of the chemotherapy drugs used in this study have been documented to induce reactive oxygen species in many tissues including the CNS [27, 34–36]. GPX1 (glutathione peroxidase) is an intracellular antioxidant enzyme that catalyzes the reduction of hydrogen peroxide (H_2O_2) by glutathione to buffer cells against oxidative damage. Similarly, PRDX1 (peroxiredoxin 1) has an important role in the detoxification of peroxides. Therefore, the upregulation of the antioxidant defenses indicates a response to oxidative stress induced by systemic treatment with the combination AC-chemotherapy.

The mitogen-activated protein kinases (MAPKs) comprise a large family of protein kinases that include the extracellular signal regulated kinases- ERK1/ERK2 (p44MAPK/ p42MAPK), the c-Jun N-terminal kinases (JNKs) and p38 MAPKs [37]. These signaling molecules play an important role in relaying extracellular signals from the cellular membrane to the nucleus through a cascade of phosphorylation events. There has been significant interest in the redox regulation of these pathways due to the role of MAPK signaling in the mediation of both mitogen- and stress-activated signals. Furthermore, the MAPK signaling pathways are implicated in the pathogenesis of many neurodegenerative diseases and cancers [38]. Our study shows that the robust activation of the ERK1/2 and SAPK/JNK signaling pathways and the expression of their direct substrates p90 RSK and phosphorylated c-Jun were detected in the hippocampus of chemotherapy treated rats. These results suggest that chronic activation of the observed signaling molecules could be related to oxidative stress and inflammatory conditions in the CNS imposed by systemic AC chemotherapy. Although not examined in this study, p38 MAPK is another signaling cascade that is associated with the neurotoxicity of chemotherapeutic agents [39]. Future studies will address the contributions of different signaling pathways in the effects of chemotherapy in the brain.

The antineoplastic agents used in the study are generally associated with oxidative DNA damage. Here, we report that systemic chemotherapy induces prominent oxidation of RNA in the hippocampus. 8-Hydroxyguanosine (8-OHG) is a common base modification found in RNA and is typically assessed as a stable biomarker for oxidative damage [40]. In this study, we adapted a novel approach to examine the consequences of chemotherapy on the oxidative modifications of nucleic acids in the brain. Specifically, relatively higher levels of the modified ribonucleotide guanine were detected in 18S and 28S ribosomal RNA (rRNA) obtained from fractionated total RNA of chemotherapy treated groups. Interestingly, the immunohistochemical data demonstrates that the extent of 8-OHG localization in the hippocampus is prominent in cytoplasmic regions, suggesting that RNA is a major target of modification. This observation is further supported by the results of the immuno-Northern

Blot (INB) experiments with RNA samples that were processed with DNAse enzyme to remove contaminating nDNA. High levels of rRNA oxidation could induce ribosome dysfunction and impair translational processes, which may play a role in the development of CRCI [41]. It will be necessary to examine the effects of treatment on the oxidation status of other RNA species (e.g. mRNA, other non-coding RNA) and to address whether specific gene transcripts are selectively targeted by oxidative damage [42, 43].

A mechanism for the toxic effects of doxorubicin are related to the ability of the chemotherapeutic agent to generate free radicals. Higher signal intensities of the DNA/RNA oxidative damage marker 8-OH(d)G was observed in neurons after doxorubicin treatment (Fig. 7c). The use of primary neuronal cells is a powerful tool for investigating mechanisms of neurotoxicity and provides a reliable model to study disease and neurodevelopment. Most studies using primary neurons are derived from embryonic or early postnatal brains to provide a homogenous neuronal population and reduce contamination from astrocyte and microglial cell subsets. Although possible, it is technically difficult to cultivate and maintain long -term cultures of neurons from discrete regions in the adult or aged brain. Furthermore, cultured embryonic and adult- derived neurons demonstrate similar electrophysiological properties [48, 49]. We found that Dox increased the overall levels of ROS and superoxide anions that were detected in the cytoplasm and neurites of the hippocampal neurons (Fig. 7a, b). Furthermore, ROS signals were mitigated in the cells by pre-exposure to the antioxidant acetyl-L- carnitine (ALCAR). Long term dietary administration of a range of pharmacological agents including ALCAR, N-acetylcysteine and plant phytochemicals have been utilized as antioxidant strategies for reducing ROS production and slowing the onset of age related cognitive deficits [36, 39]. Future studies could utilize long-term cultured neurons as this *in vitro* senescent model recapitulates many features of aging including protein nitration, mitochondrial dysfunction and senescence-associated beta-galactosidase expression. It is expected that aged neurons would be more susceptible to the oxidative damage induced by chemotherapy exposure.

Cancer and cancer- related treatment is associated with psychosocial and physiological stress. The concomitant structural and functional changes observed in patients likely involve alterations in gene expression that influence cognitive processes in the brain. Taken together, our data demonstrate that chemotherapy leads to an induction of inflammatory genes and stress signaling proteins in the hippocampus of rats, biomarkers that are also related to the processes of brain aging. Thus, chemotherapy may have a direct impact on the brain and accelerate aging. In our most vulnerable populations, this impact may have a more profound consequence in cognitive dysfunction and may partially explain the heterogeneity of the severity of impairment. Furthermore, we established the first evidence that systemic delivery of these cytotoxic agents can induce oxidative damage to RNA in the brain, which may ultimately play a role in the pathophysiology of cognitive impairment after treatment. This novel information will help in the identification of pharmacological interventions for the amelioration of cognitive impairment induced by chemotherapy.

Funding:

The authors wish to thank funding: NIH/NCI grant U54CA132378 and U54 CA137788 to TA, KSR and KH; NIH/RISEGM08168 grant to CB; NIH/RCMI grant 5G12MD007603 to KH and KSR.

References

1. Cupit-Link MC, Kirkland JL, Ness KK, et al. (2017) Biology of premature ageing in survivors of cancer. ESMO Open 2:e000250 10.1136/esmoopen-2017-000250 [PubMed: 29326844]
2. Sanoff HK, Deal AM, Krishnamurthy J, et al. (2014) Effect of cytotoxic chemotherapy on markers of molecular age in patients with breast cancer. J Natl Cancer Inst 106:dju057 10.1093/jnci/dju057 [PubMed: 24681605]
3. Koppelmans V, Breteler MMB, Boogerd W, et al. (2012) Neuropsychological Performance in Survivors of Breast Cancer More Than 20 Years After Adjuvant Chemotherapy. J Clin Oncol 30:1080–1086. 10.1200/JCO.2011.37.0189 [PubMed: 22370315]
4. de Ruiter MB, Reneman L, Boogerd W, et al. (2011) Cerebral hyporesponsiveness and ognitive impairment 10 years after chemotherapy for breast cancer. Hum Brain Mapp 32:1206–1219. 10.1002/hbm.21102 [PubMed: 20669165]
5. Ahles TA, Saykin AJ (2007) Candidate mechanisms for chemotherapy-induced cognitive changes. Nat Rev Cancer 7:192–201. 10.1038/nrc2073 [PubMed: 17318212]
6. Wang X-M, Walitt B, Saligan L, et al. (2015) Chemobrain: A critical review and causal hypothesis of link between cytokines and epigenetic reprogramming associated with chemotherapy. Cytokine 72:86–96. 10.1016/j.cyto.2014.12.006 [PubMed: 25573802]
7. Seigers R, Fardell JE (2011) Neurobiological basis of chemotherapy-induced cognitive impairment: A review of rodent research. Neurosci Biobehav Rev 35:729–741. 10.1016/j.neubiorev.2010.09.006 [PubMed: 20869395]
8. Kaiser J, Bledowski C, Dietrich J (2014) Neural correlates of chemotherapy-related cognitive impairment. Cortex 54:33–50. 10.1016/j.cortex.2014.01.010 [PubMed: 24632463]
9. Janelsins MC, Kesler SR, Ahles TA, Morrow GR (2014) Prevalence, mechanisms, and management of cancer-related cognitive impairment. Int Rev Psychiatry 26:102–113. 10.3109/09540261.2013.864260 [PubMed: 24716504]
10. Greene J, Hennessy B (2015) The role of anthracyclines in the treatment of early breast cancer. J Oncol Pharm Pract 21:201–212. 10.1177/1078155214531513 [PubMed: 24769570]
11. Yang F, Kemp CJ, Henikoff S (2015) Anthracyclines induce double-strand DNA breaks at active gene promoters. Mutat Res 773:9–15. 10.1016/j.mrfmmm.2015.01.007 [PubMed: 25705119]
12. Sterba M, Popelova O, Vavrova A, et al. (2013) Oxidative stress, redox signaling, and metal chelation in anthracycline cardiotoxicity and pharmacological cardioprotection. Antioxid Redox Signal 18:899–929. 10.1089/ars.2012.4795 [PubMed: 22794198]
13. Mills PJ, Ancoli-Israel S, Parker B, et al. (2008) Predictors of inflammation in response to anthracycline-based chemotherapy for breast cancer. Brain Behav Immun 22:98–104. 10.1016/j.bbi.2007.07.001 [PubMed: 17706918]
14. Janelsins MC, Mustian KM, Palesh OG, et al. (2012) Differential expression of cytokines in breast cancer patients receiving different chemotherapies: implications for cognitive impairment research. Support Care Cancer 20:831–839. 10.1007/s00520-011-1158-0 [PubMed: 21533812]
15. McDonald BC, Conroy SK, Ahles TA, et al. (2012) Alterations in Brain Activation During Working Memory Processing Associated With Breast Cancer and Treatment: A Prospective Functional Magnetic Resonance Imaging Study. J Clin Oncol 30:2500–2508. 10.1200/JCO.2011.38.5674 [PubMed: 22665542]
16. Kesler SR, Blayney DW (2016) Neurotoxic Effects of Anthracycline- vs Nonanthracycline-Based Chemotherapy on Cognition in Breast Cancer Survivors. JAMA Oncol 2:185 10.1001/jamaoncol.2015.4333 [PubMed: 26633037]
17. Dietrich J, Prust M, Kaiser J (2015) Chemotherapy, cognitive impairment and hippocampal toxicity. Neuroscience 309:224–232. 10.1016/j.neuroscience.2015.06.016 [PubMed: 26086545]

18. Seigers R, Schagen SB, Van Tellingen O, Dietrich J (2013) Chemotherapy-related cognitive dysfunction: current animal studies and future directions. Brain Imaging Behav 7:453–459. 10.1007/s11682-013-9250-3 [PubMed: 23949877]
19. Christie L-A, Acharya MM, Parihar VK, et al. (2012) Impaired cognitive function and hippocampal neurogenesis following cancer chemotherapy. Clin Cancer Res Off J Am Assoc Cancer Res 18:1954–1965. 10.1158/1078-0432.CCR-11-
20. Ren X, St Clair DK, Butterfield DA (2017) Dysregulation of cytokine mediated chemotherapy induced cognitive impairment. Pharmacol Res 117:267–273. 10.1016/j.phrs.2017.01.001 [PubMed: 28063894]
21. Shi D-D, Huang Y-H, Lai CSW, et al. (2018) Chemotherapy-Induced Cognitive Impairment Is Associated with Cytokine Dysregulation and Disruptions in Neuroplasticity. Mol Neurobiol. 10.1007/s12035-018-1224-4
22. Aluise CD, Miriyala S, Noel T, et al. (2011) 2-Mercaptoethane sulfonate prevents doxorubicin-induced plasma protein oxidation and TNF-α release: Implications for the reactive oxygen species-mediated mechanisms of chemobrain. Free Radic Biol Med 50:1630–1638. 10.1016/j.freeradbiomed.2011.03.009 [PubMed: 21421044]
23. Gaman AM, Uzoni A, Popa-Wagner A, et al. (2016) The Role of Oxidative Stress in Etiopathogenesis of Chemotherapy Induced Cognitive Impairment (CICI)-"Chemobrain". Aging Dis 7:307–317. 10.14336/AD.2015.1022 [PubMed: 27330845]
24. Salas-Ramirez KY, Bagnall C, Frias L, et al. (2015) Doxorubicin and cyclophosphamide induce cognitive dysfunction and activate the ERK and AKT signaling pathways. Behav Brain Res 292:133–141. 10.1016/j.bbr.2015.06.028 [PubMed: 26099816]
25. Francis PA, Regan MM, Fleming GF, et al. (2015) Adjuvant ovarian suppression in premenopausal breast cancer. N Engl J Med 372:436–446. 10.1056/NEJMoa1412379 [PubMed: 25495490]
26. Wang X, Michaelis EK (2010) Selective neuronal vulnerability to oxidative stress in the brain. Front Aging Neurosci 2:12 10.3389/fnagi.2010.00012 [PubMed: 20552050]
27. Joshi G, Aluise CD, Cole MP, et al. (2010) Alterations in brain antioxidant enzymes and redox proteomic identification of oxidized brain proteins induced by the anti-cancer drug adriamycin: implications for oxidative stress-mediated chemobrain. Neuroscience 166:796–807. 10.1016/j.neuroscience.2010.01.021 [PubMed: 20096337]
28. Tangpong J, Cole MP, Sultana R, et al. (2006) Adriamycin-induced, TNF-alpha-mediated central nervous system toxicity. Neurobiol Dis 23:127–139. 10.1016/j.nbd.2006.02.013 [PubMed: 16697651]
29. Aluise CD, Sultana R, Tangpong J, et al. (2010) Chemo brain (chemo fog) as a potential side effect of doxorubicin administration: role of cytokine-induced, oxidative/nitrosative stress in cognitive dysfunction. Adv Exp Med Biol 678:147–156 [PubMed: 20738017]
30. Weber MT, Maki PM, McDermott MP (2014) Cognition and mood in perimenopause: a systematic review and meta-analysis. J Steroid Biochem Mol Biol 142:90–98. 10.1016/j.jsbmb.2013.06.001 [PubMed: 23770320]
31. Kitamura Y, Hattori S, Yoneda S, et al. (2015) Doxorubicin and cyclophosphamide treatment produces anxiety-like behavior and spatial cognition impairment in rats: Possible involvement of hippocampal neurogenesis via brain-derived neurotrophic factor and cyclin D1 regulation. Behav Brain Res 292:184–193. 10.1016/j.bbr.2015.06.007 [PubMed: 26057360]
32. Kesler S, Janelsins M, Koovakkattu D, et al. (2013) Reduced hippocampal volume and verbal memory performance associated with interleukin-6 and tumor necrosis factor-alpha levels in chemotherapy-treated breast cancer survivors. Brain Behav Immun 30 Suppl:S109–116. 10.1016/j.bbi.2012.05.017 [PubMed: 22698992]
33. Hayslip J, Dressler EV, Weiss H, et al. (2015) Plasma TNF-alpha and Soluble TNF Receptor Levels after Doxorubicin with or without Co-Administration of Mesna-A Randomized, Cross-Over Clinical Study. PloS One 10:e0124988 10.1371/journal.pone.0124988 [PubMed: 25909710]
34. Oboh G, Akomolafe TL, Adefegha SA, Adetuyi AO (2011) Inhibition of cyclophosphamide-induced oxidative stress in rat brain by polar and non-polar extracts of Annatto (Bixa orellana) seeds. Exp Toxicol Pathol Off J Ges Toxikol Pathol 63:257–262. 10.1016/j.etp.2010.01.003

35. Ince S, Kucukkurt I, Demirel HH, et al. (2014) Protective effects of boron on cyclophosphamide induced lipid peroxidation and genotoxicity in rats. Chemosphere 108:197–204. 10.1016/j.chemosphere.2014.01.038 [PubMed: 24530163]
36. El-Agamy SE, Abdel-Aziz AK, Wahdan S, et al. (2018) Astaxanthin Ameliorates Doxorubicin-Induced Cognitive Impairment (Chemobrain) in Experimental Rat Model: Impact on Oxidative, Inflammatory, and Apoptotic Machineries. Mol Neurobiol 55:5727–5740. 10.1007/s12035-017-0797-7 [PubMed: 29039023]
37. Morrison DK (2012) MAP kinase pathways. Cold Spring Harb Perspect Biol 4:. 10.1101/cshperspect.a011254
38. Kim EK, Choi E-J (2010) Pathological roles of MAPK signaling pathways in human diseases. Biochim Biophys Acta 1802:396–405. 10.1016/j.bbadis.2009.12.009 [PubMed: 20079433]
39. Liu R-Y, Zhang Y, Coughlin BL, et al. (2014) Doxorubicin attenuates serotonin-induced long-term synaptic facilitation by phosphorylation of p38 mitogen-activated protein kinase. J Neurosci Off J Soc Neurosci 34:13289–13300. 10.1523/JNEUROSCI.0538-14
40. Poulsen HE, Specht E, Broedbaek K, et al. (2012) RNA modifications by oxidation: a novel disease mechanism? Free Radic Biol Med 52:1353–1361. 10.1016/j.freeradbiomed.2012.01.009 [PubMed: 22306201]
41. Simms CL, Zaher HS (2016) Quality control of chemically damaged RNA. Cell Mol Life Sci CMLS 73:3639–3653. 10.1007/s00018-016-2261-7 [PubMed: 27155660]
42. Kong Q, Lin C-LG (2010) Oxidative damage to RNA: mechanisms, consequences, and diseases. Cell Mol Life Sci CMLS 67:1817–1829. 10.1007/s00018-010-0277-y [PubMed: 20148281]
43. Nunomura A, Lee H-G, Zhu X, Perry G (2017) Consequences of RNA oxidation on protein synthesis rate and fidelity: implications for the pathophysiology of neuropsychiatric disorders. Biochem Soc Trans 45:1053–1066. 10.1042/BST20160433 [PubMed: 28778984]
44. Salas-Ramirez KY, Bagnall C, Frias L, et al. (2015) Doxorubicin and cyclophosphamide induce cognitive dysfunction and activate the ERK and AKT signaling pathways. Behav Brain Res 292:133–141. 10.1016/j.bbr.2015.06.028 [PubMed: 26099816]
45. Mishima E, Jinno D, Akiyama Y, et al. (2015) Immuno-Northern Blotting: Detection of RNA Modifications by Using Antibodies against Modified Nucleosides. PloS One 10:e0143756 10.1371/journal.pone.0143756 [PubMed: 26606401]
46. Brown T, Mackey K, Du T (2004) Analysis of RNA by northern and slot blot hybridization. Curr Protoc Mol Biol Chapter 4:Unit 4.9. 10.1002/0471142727.mb0409s67
47. Brewer GJ, Torricelli JR, Evege EK, Price PJ (1993) Optimized survival of hippocampal neurons in B27-supplemented Neurobasal, a new serum-free medium combination. J Neurosci Res 35:567–576. 10.1002/jnr.490350513 [PubMed: 8377226]
48. Evans MS, Collings MA, Brewer GJ (1998) Electrophysiology of embryonic, adult and aged rat hippocampal neurons in serum-free culture. J Neurosci Methods 79:37–46. [PubMed: 9531458]
49. Bushell TJ, Lee CC, Shigemoto, Miller RJ (1999) Modulation of synaptic transmission and differential localisation of mGlus in cultured hippocampal autapses. Neuropharmacology 38:1553–1567. [PubMed: 10530817]

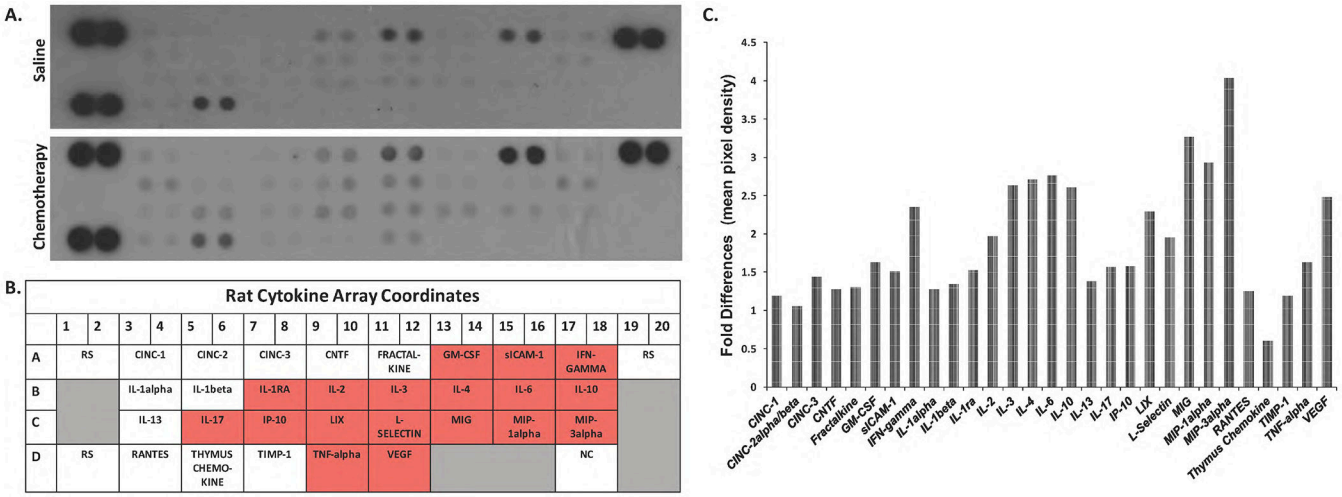

	1	2	3	4	5	6	7	8	9	10	11	12	13	14	15	16	17	18	19	20
A	RS		CINC-1		CINC-2		CINC-3		CNTF		FRACTAL-KINE		GM-CSF		sICAM-1		IFN-GAMMA		RS	
B			IL-1alpha		IL-1beta		IL-1RA		IL-2		IL-3		IL-4		IL-6		IL-10			
C			IL-13		IL-17		IP-10		LIX		L-SELECTIN		MIG		MIP-1alpha		MIP-3alpha			
D	RS		RANTES		THYMUS CHEMO-KINE		TIMP-1		TNF-alpha		VEGF						NC			

Fig. 1:

Cytokine and chemokine production was evaluated using Proteome Profiler arrays (R&D Systems) as described in *Materials* and *Methods*. **a)** Representative cytokine panel of protein lysates prepared from the hippocampus of saline or AC chemotherapy-treated rats (n=6). Membranes shown are from a 10-minute exposure to x-ray film. **b)** Cytokine/chemokine array duplicate spot coordinates (red: >1.5- fold upregulation in protein expression compared to saline-control). RS, reference spots; NC, negative controls. **c)** Densitometric analyses of the antibody arrays. The mean pixel density of the cytokine/chemokine spots was divided by the mean pixel density of the reference spots for each membrane. The column graphs display the fold changes of AC chemotherapy groups compared to saline controls.

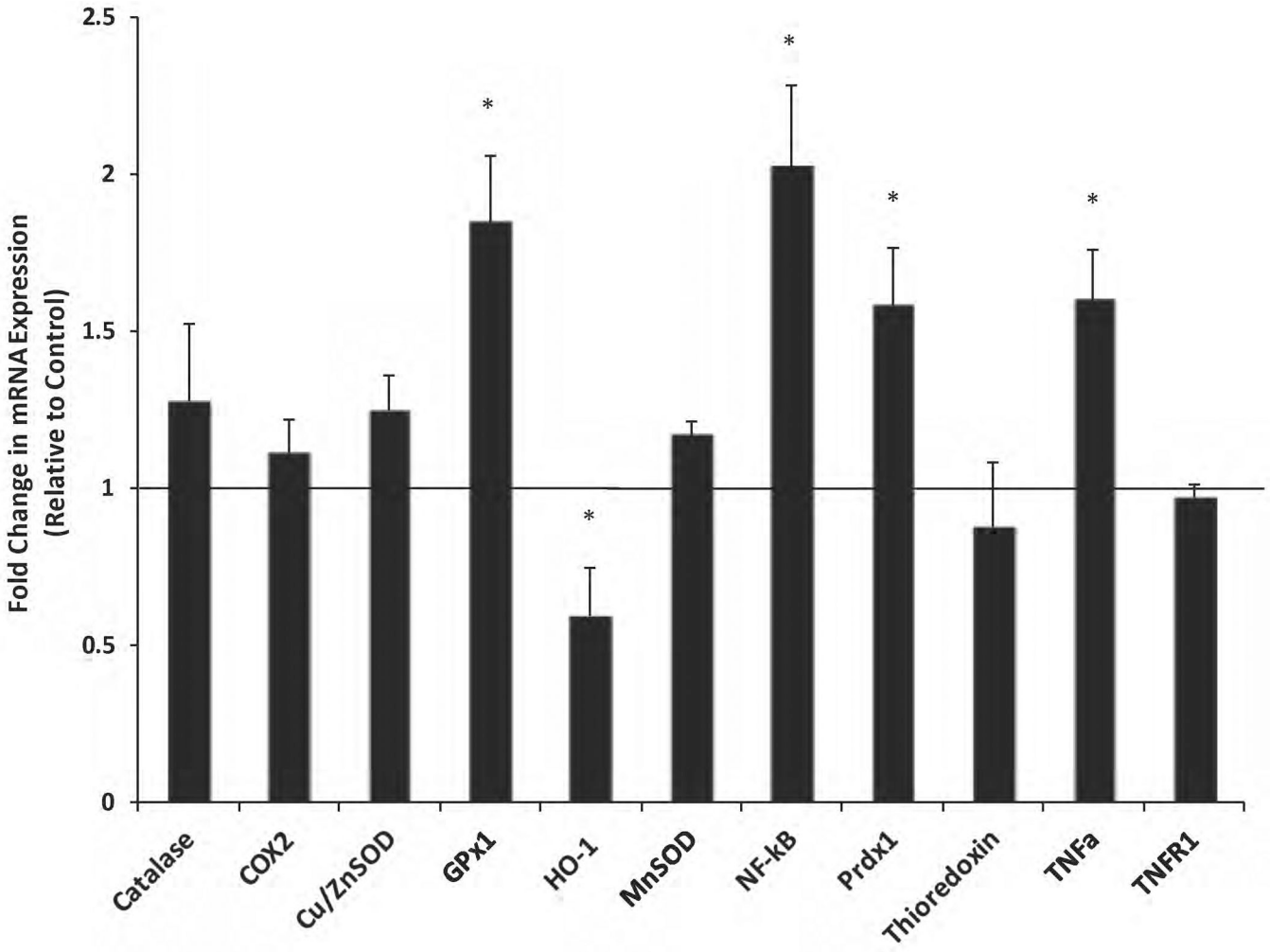

Fig. 2:

Analysis of oxidative stress -responsive gene expression by qRT-PCR in the hippocampus of rats after chemotherapy treatment. The relative mRNA expression of genes related to oxidative stress were evaluated in the hippocampus of AC chemotherapy treated rats compared to saline controls. Fold changes were quantified using the $2^{-\Delta\Delta Ct}$ method and normalized to the levels of GAPDH. Error bars denote SEM. * $p < 0.05$ vs saline group.

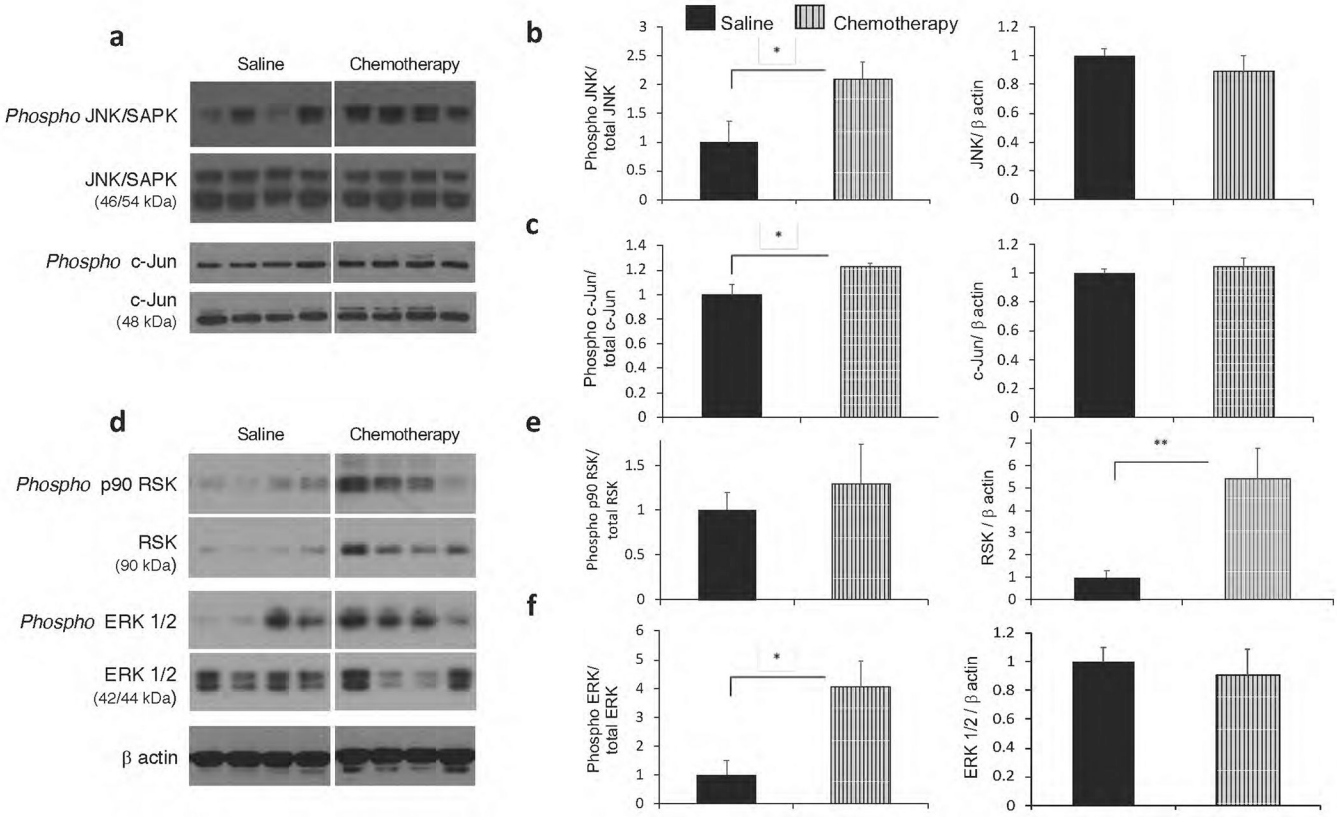

Fig. 3:

Elevated JNK/SAPK and ERK/MAPK signaling in the hippocampus after chemotherapy. **a)** Representative immunoblots showing expression of p JNK/SAPK, total JNK/SAPK, p c-Jun, and total c-Jun from saline (n=6) and chemotherapy (n=7) groups. Blots were normalized to total JNK (p JNK), total c-Jun (p c-Jun) or β-actin (JNK/SAPK and c-Jun) **b)** Quantification of the immunoblot signals for p JNK/SAPK demonstrate a significant increase in activation among chemotherapy groups. No differences observed in total JNK/SAPK expression. **b)** Quantification of the immunoblot signals for p c-Jun demonstrate a significant increase in activation among chemotherapy groups relative to saline-control groups. No differences observed in total c- Jun expression. **d)** Representative immunoblots showing expression of p RSK, total RSK, p ERK 1/2, and total ERK 1/2 from saline (n=6) and chemotherapy (n=7) groups. Blots were normalized to total RSK (p RSK), total ERK1/2 (p ERK 1/2) or β-actin (RSK and ERK1/2) **e)** Quantification of the immunoblot signals for p RSK show that there were no differences in the relative levels of phosphorylated RSK protein (ratio of p RSK/ total RSK) among the groups. Significant increases in total RSK protein expression was observed in chemotherapy groups. **f)** Quantification of the immunoblot signals for p ERK1/2 demonstrate a significant increase in activation among chemotherapy groups relative to saline-control groups. No differences observed in total ERK 1/2 expression. *p< 0.05, **p< 0.005 vs. saline group; *n.s.*, no significance.

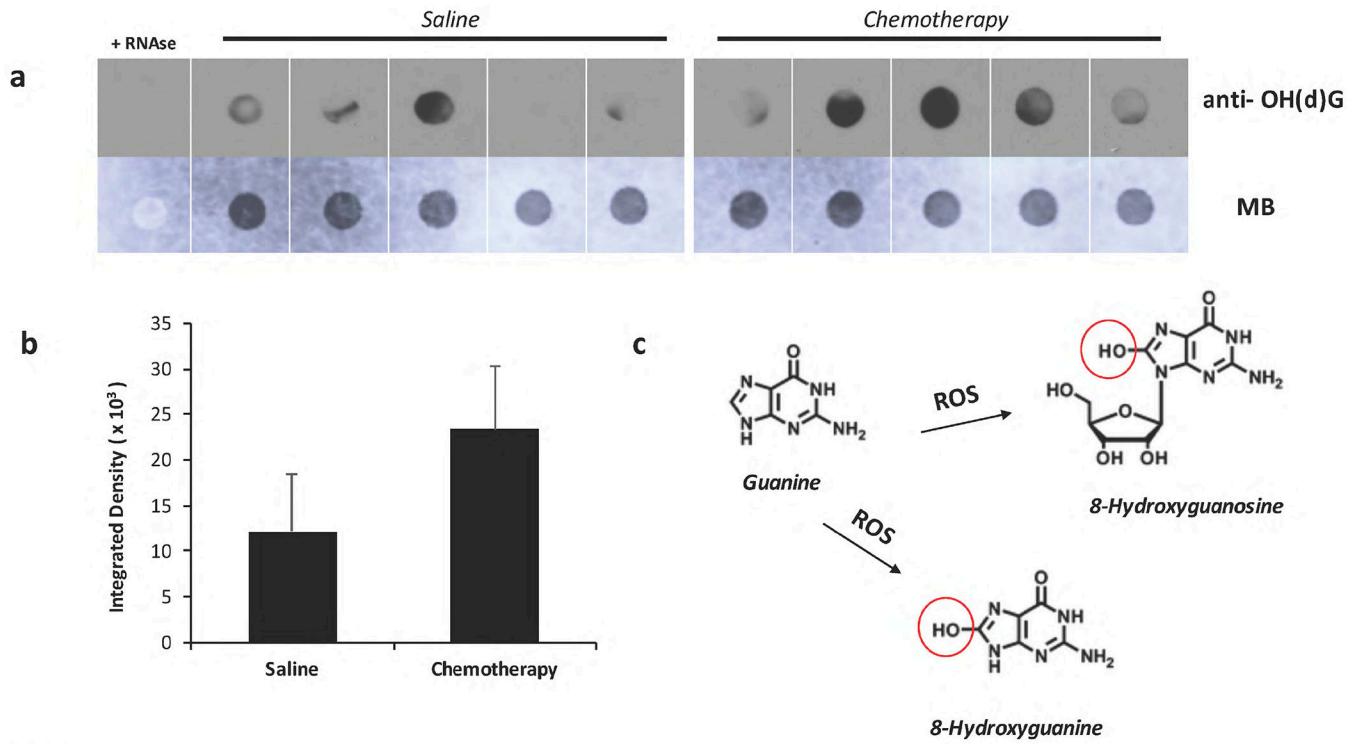

Fig. 4:

a) Immuno-dot blot analysis of unfractionated total RNA from the hippocampus of saline or chemotherapy treated animals for the detection of 8-Hydroxyguanosine (8-OH(d)G). The same blot is shown in the lower panel and equal loading of total RNA was verified by methylene blue staining. **b)** Semi-quantitative analysis of oxidized RNA by densitometry. A relative increase in 8-OH(d)G immunoreactivity was found in chemotherapy groups, although this difference was not statistically significant. **c)** Reactive oxygen species oxidize guanine and generates 8-oxo-7,8-dihydroguanine or 8-oxo-7,8-dihydroguanosine (8-OHG) in RNA. For negative control, samples were treated with RNAse as described in *Materials and Methods*.

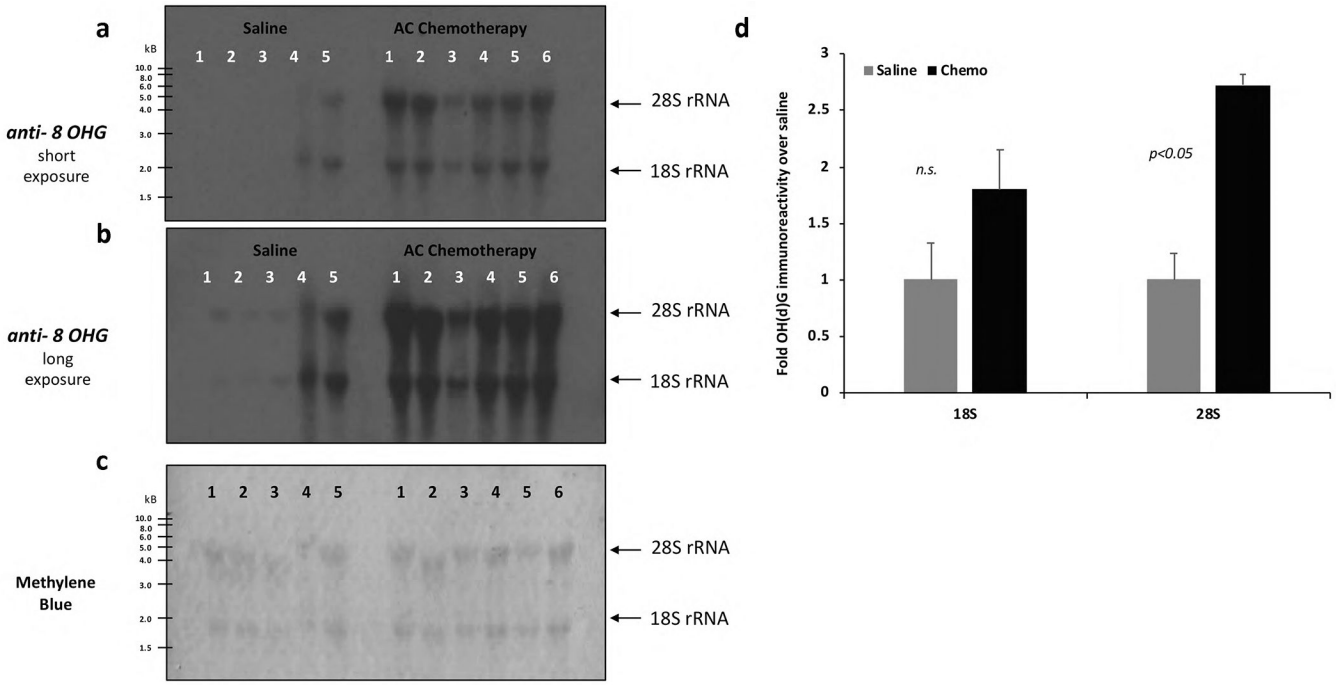

Fig. 5:

Total RNA (2 μg) isolated from the hippocampus was analyzed by INB (Immuno-Northern Blot) with the anti-OH(d)G antibody after electrophoresis in 1% agarose denaturing gel (*Materials and Methods*). Long exposures **(a)** and short exposures **(b)** of the INB are displayed. **c)** Equal loading of RNA was assessed by methylene blue staining. Chemotherapy treated animals (n=6) have significantly higher levels of oxidized 28S ribosomal RNA bands than saline- controls (n=5) **(d)**. Densitometric analysis was performed to quantitate the band intensities. Data were expressed relative to the band intensity of saline groups. Values are shown as the mean ± SEM. *$p < 0.05$ vs. saline group; *n.s., no significance*.

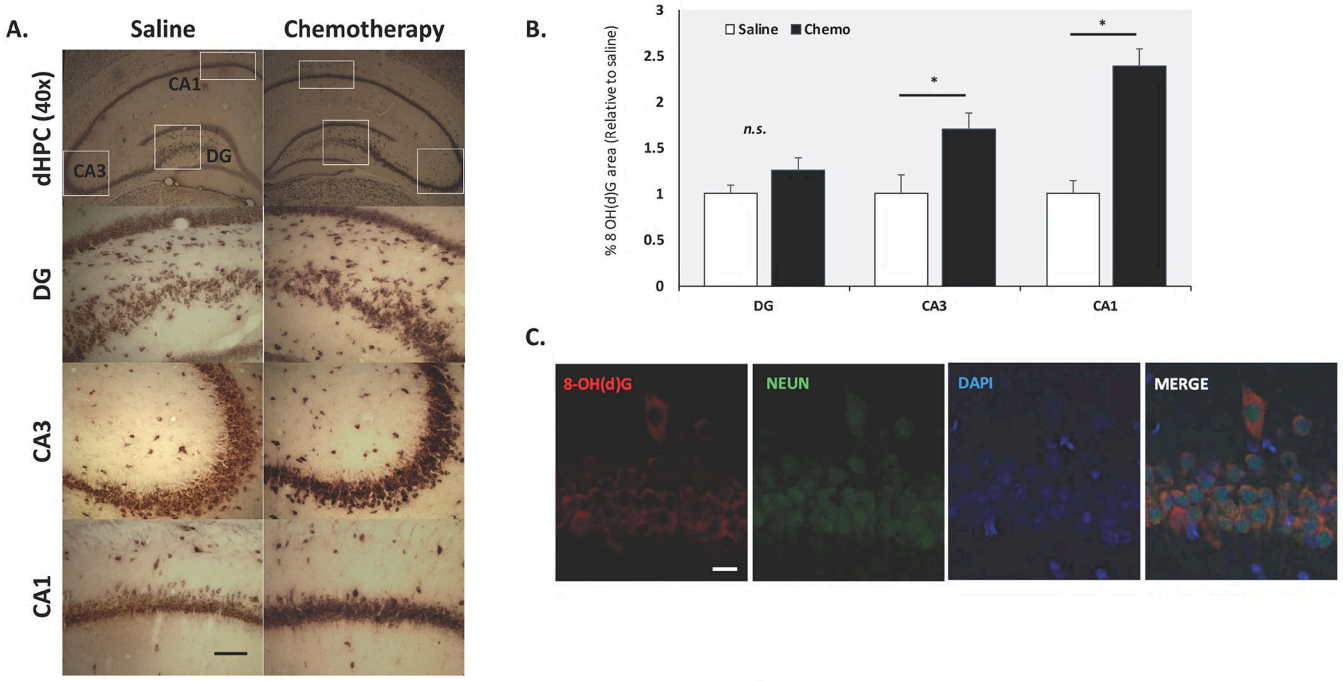

Fig. 6:

Representative photomicrograph of 8-oxo-7,8-dihydroguanosine (8-OHG)/ 8-oxo-7,8-dihydro-2-deoxyguanosine (8-OHdG) immunohistochemistry in the dentate gyrus (DG), CA3 and CA1 regions of the dHPC (dorsal hippocampus) in saline and chemo-treated rats. Scale bar :100 mm; Magnification: 40x; 200x **(a).** In chemo-treated animals, increased neuronal staining for 8-OHdG was observed in the hippocampal brain regions. Semi-quantitative image analysis of 8-OHdG staining intensity as described in Materials and Methods **(b).** Double immunofluorescence of hippocampal tissue sections with antibodies specific to NEUN demonstrate 8-OH(d)G labeling is restricted to neuronal cell types **(c)**. Data were obtained from N=5 animals per group and presented as the mean ± SEM. *p <0.05 vs. saline group

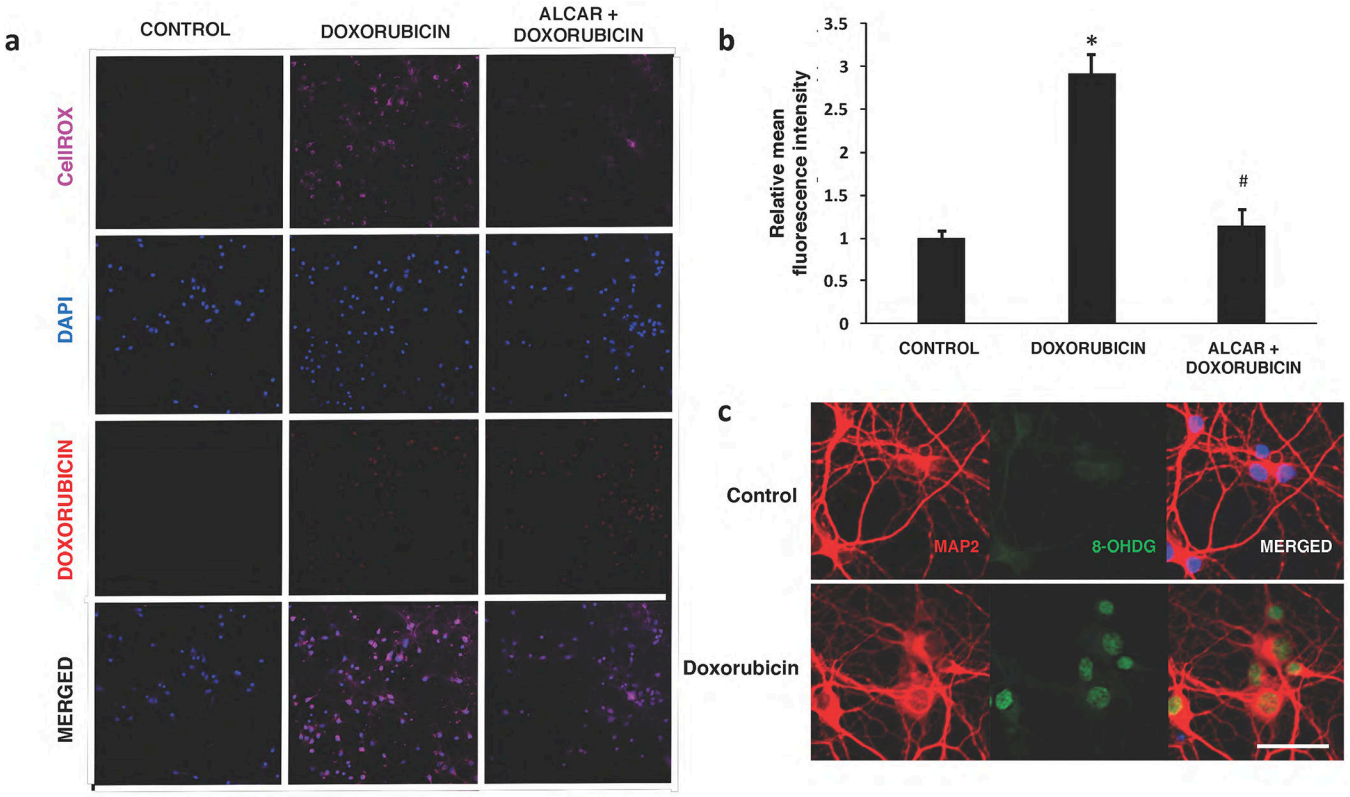

Fig. 7:

Doxorubicin induces oxidative stress in hippocampal neurons. **a)** An increase in CellROX Deep Red fluorescence was observed in Dox-treated neurons. Doxorubicin autofluorescence in the nucleus was also detected in treated neurons, but not in controls. **b)** Quantification of signal intensities demonstrate a significant increase in ROS production with Dox. Acetyl-L-carnitine (ALCAR) pre-exposure attenuates levels of ROS in doxorubicin treated cells. Data are shown as mean ± S.E.M. of 10 fields counted in duplicate from three independent experiments. *$p<0.05$ from control; $^{\#}p<0.05$ from doxorubicin- treated. **c)** Expression of the DNA oxidative damage marker 8-OHdG in hippocampal neurons.

Representative photos illustrating double immunofluorescence staining of MAP2 (red) and 8 OHdG (green) with DAPI counterstain (blue) in control (top panel) or Dox-treated (lower panel) cells. Strong positive signals for 8-OHdG were predominantly detected in the nucleus of Dox-treated neurons. Scale bar :50 μm

Table 1.

Oligonucleotide primers used in the study

Target cDNA	NCBI Reference Sequence	Primers (5′-3′) forward/ reverse
GAPDH	XM_017593963.1	TGATTCTACCCACGGCAAGTT/ TGATGGGTTTCCCATTGATGA
HO-1	NM_012580.2	GAGCGAAACAAGCAGAACCC/ ACCTCGTGGAGACGCTTTAC
CATALASE	NM_012520.2	GAGAGGAAACGCCTGTGTGA/ TTGGCAGCTATGTGAGAGCC
COX2	NM_017232.3	TGTATGCTACCATCTGGCTTCGG/ GTTTGGAACAGTCGCTCGTC
GPX1	NM_030826.4	GCTCACCCGCTCTTTACCTT/ GATGTCGATGGTGCGAAAGC
NFKB p65	NM_199267.2	TGGACGATCTGTTTCCCCTC/ CCCTCGCACTTGTAACGGAA
PRDXN1	BC058450.1	GGCACGTCTTCCTGTGTTCT/ TTGAAGCTGGGAGCAGGATG
Cu/Zn SOD1	NM_017050.1	CAGCGGATGAAGAGAGGCAT/ ACGGCCAATGATGGAATGCT
MnSOD	NM_017051.2	CGGGGGCCATATCAATCACA/ GCCTCCAGCAACTCTCCTTT
THIOREDOXIN	BC058454.1	AGGTTGGGGAGTTCTCTGGT/ TGGAGCTGGTCACACTTTTCA
TNFa	NM_012675.3	CCAGGAGAAAGTCAGCCTCCT/ TCATACCAGGGCTTGAGCTCA
TNFR1	NM_013091.1	AAGTGCCACAAAGGAACCTACT/ ACACACCTCGCAGACTGTTT